

# The galactic double-mode Cepheids

## I. Frequency analysis of the light curves and comparison with single-mode Cepheids

I. Pardo<sup>1</sup> and E. Poretti<sup>2</sup>

<sup>1</sup> Università di Milano, I-20100 Milano, Italy

<sup>2</sup> Osservatorio Astronomico di Brera, Via Bianchi 46, I-22055 Merate, Italy  
E-mail: poretti@merate.mi.astro.it

Received date; Accepted Date

**Abstract.** We submitted the available photometric  $V$  data of all the known galactic Double Mode Cepheids (DMCs) to a careful frequency analysis with the aim of detecting in each case the importance of the harmonics and of the cross coupling terms. For each object, starting from different data subsets, we progressively built a homogenous set of data, checking the consistency of the results step by step. It was demonstrated that each star displays a different content, showing that no a priori fit can be applied. Up to 4 harmonics were found for the fundamental radial mode ( $F$ ); in every case, 2 harmonics were found for the first overtone radial mode ( $1O$ ). We also proceeded to a preliminar analysis of the Fourier parameters of the DMC light curves and we found a very close similarity between *i*) the light curves of the Classical Cepheids and those of the  $F$ -mode of the DMCs; *ii*) the light curves of the  $s$ -Cepheids and those of the  $1O$ -mode of the DMCs.

The analysis of DMC light curves offers the possibility of unifying the light curves of Classical and  $s$ -Cepheids. The case of the unique DMC CO Aur is also discussed.

**Key words:** Methods: data analysis - Stars: oscillations - Cepheids - Galaxy: stellar content

### 1. Introduction

The Double Mode Cepheids (DMCs) play an important role in the study of the stellar evolution. In the recent years a substantial improvement was made to reconcile the pulsational mass (i.e. the mass predicted by the pulsation law  $Q = P\sqrt{\rho}$ ), the beat mass (i.e. the mass derived

from the ratio between the observed periods) and the evolutionary mass (i.e. the mass predicted from evolutionary tracks and luminosity). The introduction of new opacities allowed theoretical studies to fill not only the large gap between the beat and pulsation masses, but also to match the evolutionary masses (Christensen-Daalsgaard & Petersen 1995).

In the same years, following the idea first expressed by Antonello et al. (1990), Mantegazza & Poretti (1992) and Poretti (1994) carefully studied the light curves of  $s$ -Cepheids by using the Fourier decomposition technique; they redefined the  $s$ -Cepheids as the stars which do not follow the Hertzsprung progression (described by the Classical Cepheids) in the space of Fourier parameters. To explain this different behaviour it was suggested that the two classes are pulsating in two different modes, i.e. the fundamental radial ( $F$ ) mode and the first overtone radial ( $1O$ ) mode, respectively. The DMCs provide the obvious laboratory where verify this suggestion can be verified since it is a well established fact that in 13 cases out of 14 the two excited modes are indeed the fundamental and the first overtone mode; the data on V371 Per (Schmidt et al. 1995), the most promising 15<sup>th</sup> candidate, are too scanty to establish its DMC nature. In the meantime, the large amount of data collected in the framework of the MA-CHO (Alcock et al. 1995) and the EROS (Beaulieu et al. 1995) projects yielded the first confirmation of the different pulsation modes since the Classical and  $s$ -Cepheids are separated in a  $P - L$  plane exactly by the shift due to the  $1O/F$  ratio. Moreover, new arguments were added to the debate owing to the large number of DMCs discovered in the LMC, against the only 14 cases observed in the Galaxy. To define in an accurate way the properties of the small number of galactic DMCs is mandatory to perform a significant comparison with the properties of the more numerous LMC DMCs.

Send offprint requests to: E. Poretti

The light curve of a DMC can be considered as the sum of the contributions of a number of frequencies, of which two only are independent ( $f_1$  and  $f_2$ ). Since each of these two curves is not, as a rule, perfectly sine-shaped, we also have to observe the  $2f_1$ ,  $3f_1$ ,  $4f_1$ , ...,  $2f_2$ ,  $2f_2$ ,  $3f_2$ ,  $4f_2$ ... harmonics; moreover, the two modes are interacting and the cross coupling terms (i.e. their combination  $|if_1 \pm jf_2|$ ; the two cases  $f_2 - f_1$ ,  $f_1 + f_2$  are the most frequent) are expected to be observed. Even if systematic photoelectric surveys of DMCs were performed from 1947 onward (TU Cas; Oosterhoof 1959), no exhaustive study of their light curves was carried out; the most complete analysis was surely the one outlined by Stobie & Balona (1979). However, in that important paper also the light curve description was made on the basis of an *a priori* choice, i.e. the application of a 2<sup>nd</sup>-order fit to the collected points. This approach was also used by Faulkner (1977) to study the light variation of U TrA: he applied three different fits (3<sup>rd</sup>, 4<sup>th</sup>, 5<sup>th</sup> order), but he did not investigate whether all the components were really present in the data, since the major result (i.e. the presence and the strength of the cross-coupling terms) is slightly affected by the completeness of the frequency content. Stobie & Balona were mainly interested in the phasing of the magnitude, colour and radial velocity observations and they showed, in the particular case of VX Pup, that the effect of additional high-order terms was to change only slightly the amplitude and the phases of the low-order terms, not affecting their main result. We can conclude that *in previous works no attempt was done to detect how many harmonics of  $f_1$  and  $f_2$  are necessary to fit the observed light curves and which cross coupling terms are excited by their interaction*. More recently, this incomplete approach was used by Matthews et al. (1992) in reexamining the TU Cas data: a 4<sup>th</sup>-order fit was *a priori* applied to the data, thus obtaining incorrect values for the phase parameters and inconsistent amplitude ratios (see also Poretti 1994 and Subsect. 4.4).

Therefore, it seems crucial to submit all the available photometry on DMCs to a careful frequency analysis:

1. To detect the importance of the harmonics and of the cross coupling terms for each star and to evaluate the similarities. Frequency and amplitude variations can be investigated and the search for a third independent periodicity can be carried out;
2. To compare the values of the low-order Fourier parameters with those of the galactic single-mode Cepheids. This comparison will allow us to establish the communalities between the two classes and to give an independent confirmation of the different pulsation mode observed in single-mode Cepheids;
3. To establish the properties of the Fourier parameters by determining boundary values in order to compare observed and theoretical light curves;
4. To search for the signature of resonances between modes in the Fourier parameter progression.

The first two items are discussed in this paper, the last two will be in a successive paper (Poretti & Pardo 1996; Paper II).

## 2. Light curve content detection

In our approach to the light curve analysis we did not select any arbitrary order of the fit, as in the above mentioned cases, but we searched for the terms (which would be independent frequencies, harmonics or cross coupling terms) really constituting the DMC light curve. To do this, we used the least-squares power spectrum method (Vanicek 1971) since it allows us to detect one by one the constituents of the light curves. We currently apply this algorithm to multiperiodic  $\delta$  Sct stars and in the past we already applied it to the frequency analysis of the DMC CO Aur (Antonello et al. 1986) and EW Sct (Figer et al. 1991). As a final step we fitted the observed magnitudes by means of the formula

$$V(t) = V_o + \sum_z A_z \cos[2\pi f_z(t - T_o) + \phi_z] \quad (1)$$

where  $f_z$  is the generic frequency, which can be an independent frequency ( $f_1$  and  $f_2$ ), a harmonic or a cross coupling term.

Let us discuss the methodology in detail, step by step, by anticipating the analysis of the measurements carried out by Berdnikov on AS Cas, the latest DMC discovered. In the first power spectrum of Fig. 1 the peak at  $f_1=0.3306$  cd<sup>-1</sup> and its alias structure (i.e. the  $1-f$ ,  $f+1$ ,  $2-f$ ,  $f+2$ , ... terms) introduced by the spectral window are clearly visible. The aliases are particularly strong in this dataset since the measurements were obtained in a single site; when merging measurements obtained at two or more sites the height of the aliases will decrease. Then we introduced  $f_1$  as a known constituent searching for the second term: in the second power spectrum the  $f_2=0.4639$  cd<sup>-1</sup> term and its alias structure appeared. It is important to note that no prewhitening was done: only the frequency value  $f_1$  was considered as established (known constituent; k.c.) and in the second search the unknowns were  $V_o$ ,  $A_1$ ,  $\phi_1$ ,  $f_2$ ,  $A_2$ ,  $\phi_2$ . Before proceeding further with a new frequency search, the values of  $f_1$  and  $f_2$  were refined by a simultaneous least-squares fit and then they were introduced as k.c. in the third search, which allowed us to detect the  $f_1 + f_2$  term (third panel). Now, frequency refinement is a delicate step because the third component must always satisfy the relationship  $f_1 + f_2$ ; to do this refinement, we use the MTRAP code (Carpino et al. 1987) which keeps this relationship locked throughout the best fit search. After the refinement, we introduced the  $f_1$ ,  $f_2$ ,  $f_1 + f_2$  terms as k.c. ( $V_o$ ,  $A_1$ ,  $\phi_1$ ,  $A_2$ ,  $\phi_2$ ,  $A_{f_1+f_2}$ ,  $\phi_{f_1+f_2}$ ,  $f_3$ ,  $A_3$ ,  $\phi_3$  are the unknowns) searching for the new light curve component: we detected  $2f_1$ . Once again, the refinement was performed by keeping the  $f_1 + f_2$  and  $2f_1$  relationships locked; new frequency values were then obtained and introduced

as k.c., the fifth component  $f_2 - f_1$  was detected and so on. Following this process, we detected 11 terms and we noted that in this latter case, the highest peak is not the  $2f_2 - f_1$  term, but its alias at  $1 \text{ cd}^{-1}$  (see lower left panel of Fig. 1). This overtaking is due to the interaction between noise (the terms have an amplitude of only 11 mmag against a standard deviation of 26 mmag for the measurements) and spectral window (we were dealing here with single-site measurements). When observing this event, the exact value of the cross coupling term is considered to proceed further.

The decision to stop the term selection was taken when no more term was visible over the noise distribution, i.e. when all the terms giving a significant contribution to the light curve shape were presumably identified. In Fig. 1 the 12<sup>th</sup> panel clearly shows that no other term can be detected in a clear way as the noise distribution is quite uniform. Of course, very small amplitude terms can remain hidden in the noise level, especially when dealing with inaccurate measurements.

In the frequency analysis it also occurred, at times, that after the detection of the two frequencies, their harmonics and some coupling terms, the highest peak in the power spectrum was at (or very close to)  $1.003 \text{ cd}^{-1}$ . Two preliminary checks were performed: the first, quite obvious, step was to check that such a term would not be an exotic coupling term (or any of its aliases); the next, to check that the  $1.003 \text{ cd}^{-1}$  peak would indeed be an alias of a  $0.003 \text{ cd}^{-1}$  term. In the latter hypothesis, the peak originated from a misalignment between measurements in different subsets (or in different years within the same subset). If these two checks were unsuccessful, the fact that  $1.003 \text{ cd}^{-1}$  means 1 sidereal day/day suggested the reasonable hypothesis that it was a spurious term introduced by an instrumental and/or a methodological effect. If the frequency analysis was not terminated, the  $1.003 \text{ cd}^{-1}$  term was introduced as a known constituent, but no scientific meaning was attributed to it.

As an example, let us consider the BERD measurements performed on BQ Ser, obtained in different years; Tab. 1 lists the mean magnitudes for each year and systematic shifts are indeed observed. The importance of misalignments is emphasized by Fig. 2, where the final power spectrum (i.e. the spectrum obtained by processing the BERD measurements considering  $f_1$ ,  $f_2$ ,  $2f_1$ ,  $f_1 + f_2$ ,  $f_2 - f_1$ ,  $2f_2$ ,  $2f_1 + f_2$ ,  $3f_1$  as k.c.) is shown with and without systematic corrections: the amplitude of the peak at  $0.0025 \text{ cd}^{-1}$  in the upper panel corresponds to an amplitude of 0.014 mag; after the end-to-end alignment (just before the final fit) this peak has completely disappeared (lower panel).

### 3. Data collection and reduction

A bibliographic search for published measurements was carried out over a very long time baseline; we thus found

**Table 1.** As an example of mean magnitudes differing from one year to the next the case of the BERD measurements of BQ Ser is shown; the errors on each value are a few mmag. Owing to the small number of measurements in some years, a reliable determination of the mean magnitude can be done only in the last steps of the analysis

Year	$V_0$	N
1986	9.500	25
1988	9.499	29
1989	9.498	40
1990	9.500	20
1991	9.506	31
1992	9.515	86
1993	9.525	51
1994	9.517	85
All	9.511	367

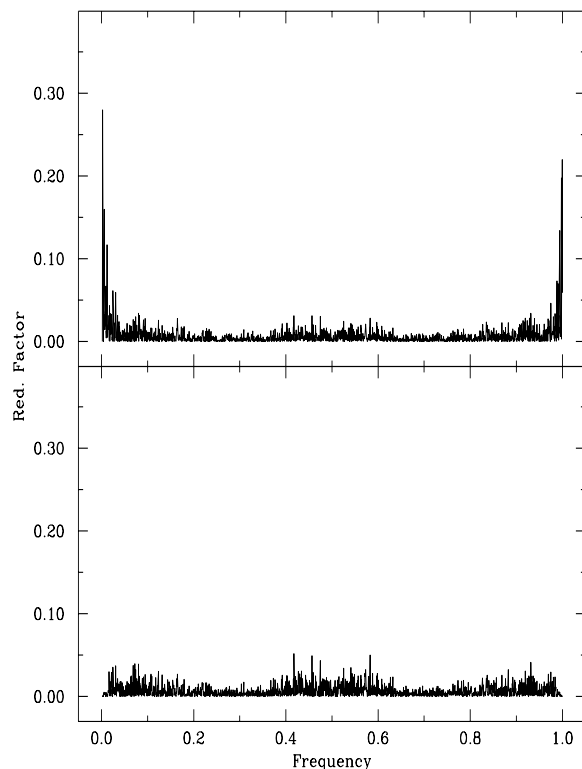


**Fig. 2.** Effects of the year-to-year misalignments in the BERD measurements of BQ Ser (upper panel: no correction; lower panel: after application of the magnitude shifts): the peaks at  $0.0$  and  $1.0 \text{ cd}^{-1}$  are strongly enhanced in the upper panel

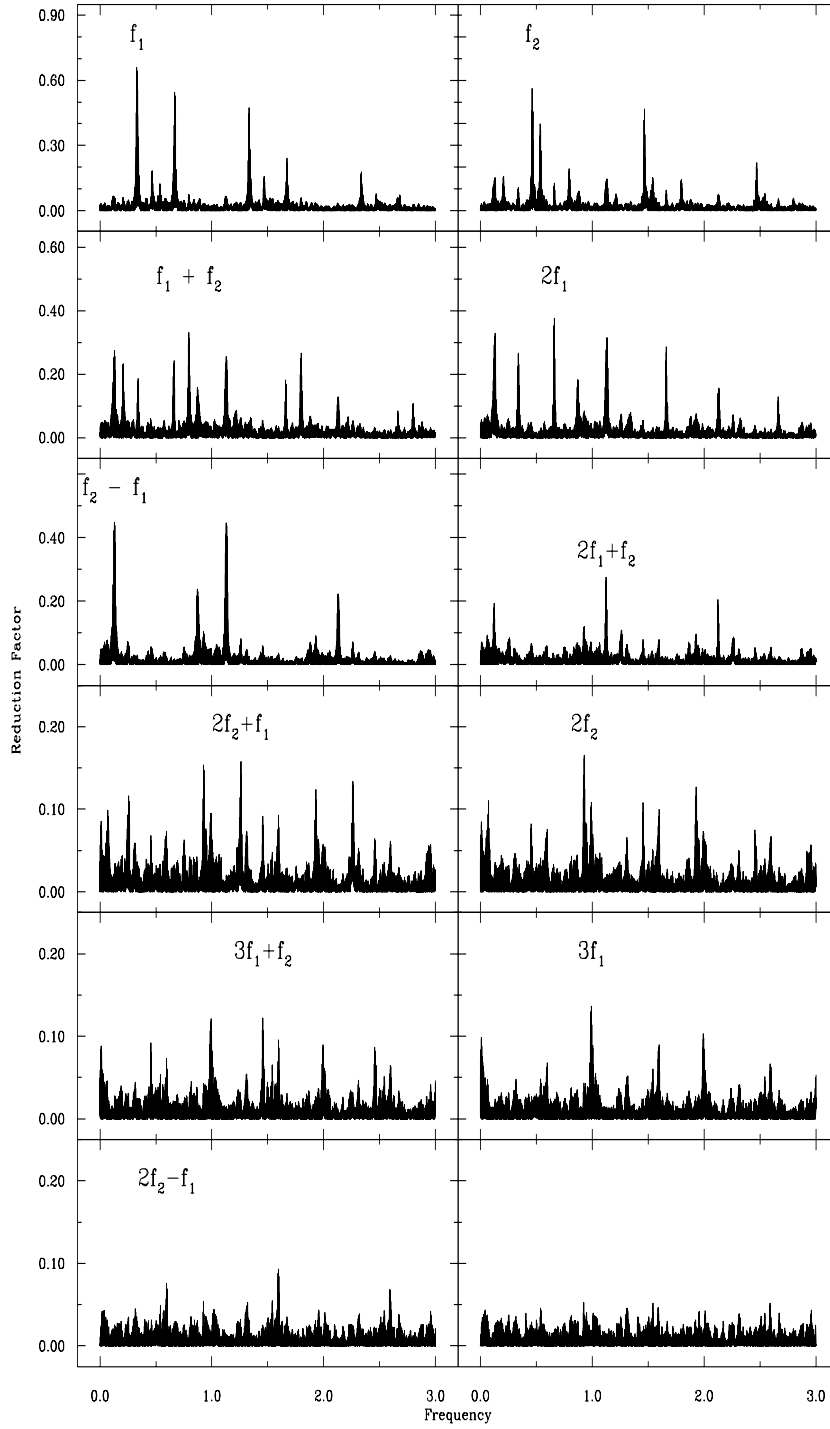


**Fig. 1.** Power spectra of the AS Cas measurements. Each panel shows the spectrum obtained by introducing all the terms identified as k.c. in the previous ones: this means that their frequencies are considered as established, but their amplitudes and phase values are recalculated for each trial frequency

**Table 2.** Double-mode Cepheid stars. AM84: Antonello & Mantegazza 1984; AM86: Antonello et al. 1986; BB87: Babel & Burki 1987; BERD: Berdnikov 1992, Berdnikov et al. 1995abc; B83: Barrell 1983; FP91: Figer et al. 1991; FS79: Faulkner & Shobbrook 1979; JA62: Jansen 1962; LJ65: Leotta Janin 1965; LTPV: Manfroid et al. 1991, 1994, Sterken et al. 1993; MI64: Mitchell et al. 1964; MS78: Madore et al. 1984; MV75: Madore & Van den Berg 1975; MB84: Moffett & Barnes 1984; OO57: Oosterhoof 1957; OO59: Oosterhoof 1959; P76: Pel 1976; SB: Stobie & Balona 1979; WE57: Worley & Eggen 1957

Star	$f_1$	$f_2$	$f_1/f_2$	$N_{\text{meas}}$	$N_{f_1}$	$N_{f_2}$	$N_{cc}$	References
TU Cas	0.467442	0.658635	0.7097	618	4	2	9	OO59 WE57 BERD
U TrA	0.389344	0.547983	0.7105	1060	4	2	6	OO57 MI64 JA62 FS79 SB79 BERD
VX Pup	0.332030	0.467384	0.7104	234	3	2	6	SB79 MB84 LTPV BERD
AS Cas	0.330628	0.463936	0.7127	575	3	2	6	BERD
AP Vel	0.319717	0.454587	0.7033	255	3	2	5	P76 SB79 BERD
BK Cen	0.315072	0.449860	0.7004	251	3	2	5	LJ65 LTPV SB79 BERD
UZ Cen	0.299910	0.424589	0.7064	131	4	2	5	P76 SB79 BERD
Y Car	0.274742	0.390698	0.7032	137	3	2	5	P76 SB 79 BERD
AX Vel	0.272241	0.385657	0.7059	520	2	2	3	BA83 P76 SB79 BERD
GZ Car	0.240448	0.340857	0.7054	118	2	2	3	P76 SB79 BERD
BQ Ser	0.234138	0.331997	0.7052	602	3	2	3	MB84 LTPV BERD
EW Sct	0.171719	0.245820	0.6986	515	3	2	3	FP91 BERD
V367 Sct	0.158902	0.228061	0.6968	514	2	3	2	MS78 MV75 BERD
CO Aur	0.560844	0.700390	0.8008	370	3	1	2	AM84 AM86 BB87 BERD

photometric data collected in a variety of systems and using both absolute (*all-sky*) and differential photometry. Since involved amplitudes are large and vary in function of the wavelength, it was considered necessary to restrict the analysis to a well defined passband. The choice of the  $V$  filter of the  $UBV(RI)$  system was quite natural since this filter was by far the most used; the  $y$  filter in the  $uvby$  photometric system was considered as equivalent. We also considered measurements carried out in other photometric systems only if the authors themselves supplied a transformation formula from his own system to the  $UBV$  one. However, the actual consistency between the  $\lambda_{\text{eq}}$  of photometric systems having different passbands is difficult to admit and also small differences can seriously affect the observed amplitudes (see the case of AX Vel).

Moreover, even if the photometric system is the same, the mean magnitude of the light variation is expected to be different. When absolute (or standard) photometry is performed, systematic differences of a few hundredths of magnitude are common in the transformation from instrumental to standard system. When differential photometry was performed, different values for the magnitude of the comparison stars were used, creating once again systematic differences.

Another serious problem was the large gaps between the different data subsets for the same star. If several years elapsed without any measurement, the data analysis was not a simple task since, for example, periods or amplitudes can change; also time series analysis are much more time-consuming (we adopted a frequency step of  $1/10\Delta t$ , where  $\Delta t$  is the difference between the times of the last and first measurements).

This being considered, we applied the following procedure to the collected measurements (the last column of Tab.2 reports the list of references):

1. We performed a very preliminary frequency analysis using the measurements reported by each author (in our terminology they constitute a *subset*), thus obtaining mean magnitude values;
2. It should be noted that a good spectral window, not only a satisfactory number of points, was necessary for our purposes. If the gaps in time were not too large, we merged two or more subsets, obtaining one or more *datasets*; to do this, we applied systematic shifts to align the subsets to the same mean magnitude level. Hence, these datasets were subject to separate frequency analysis and the components of the respective light curves were detected. In turn, the parameters of the least-squares fit were calculated;
3. In principle, the small amplitude terms detected in one dataset were not the same as the ones detected in the others and a major difficulty was to understand which of them should be considered as real. Indeed, small amplitude terms were strongly affected by the noise, different from one dataset to the other; as a result, some terms could stand out in the frequency analysis of a dataset and remain hidden in the noise of another. How could we decide which terms had to be used to describe the light curve of a DMC? To that purpose, we included the frequency of a component clearly evidenced in a dataset among the input values of a least-squares fit (*a forced fit*) of another dataset, not showing it. Therefore, we compared the phase values: if the datasets yielded similar values, the com-

ponent was considered to be significant, if not it was rejected;

4. On the basis of the previous results, all the datasets of a given DMC (and also, in some case, the subsets we could not use for the frequency analysis) were merged into the *whole set* of data, and the final least-squares fit of the data was performed, together with additional tests. In particular, we checked again the mean magnitude levels of each subset and we performed some further, minor adjustments. We also performed a frequency refinement and we reported the values we obtained in Tab. 2; the formal errors on the frequency values are of the order of a few  $10^{-6}$   $\text{cd}^{-1}$ ;
5. Once the frequency content was determined, we obtained the light curves of the two frequencies  $f_1$  and  $f_2$  by subtracting the theoretical contribution of the other terms from the measurements. To obtain the light curve on  $f_1$  we subtracted  $f_2$ ,  $2f_2$ ,  $3f_2$ , ... and all the coupling terms; to obtain the light curve on  $f_2$  we subtracted  $f_1$ ,  $2f_1$ ,  $3f_1$ , ... and again all the coupling terms.

In the next section we present a detailed description of this process as applied to the BQ Ser and AX Vel measurements. It is important to note that this process led us to perform a final fit by using all the terms detected in the power spectra and these terms only: *no a priori choice of the fit order was considered*.

To increase our confidence in the results, we also considered a different final step: before merging the datasets into the whole set of data, we determined the generalized phase differences for each dataset and then we calculated their weighted mean (this approach is fully described in Pardo 1995). The comparison between these weighted values and the ones obtained from the whole set of data showed that the two procedures yield equivalent results. Moreover, it should be also noted that from a chronological point of view, we progressively built up each set and performed several preliminar frequency analyses and fits: the stability of the amplitudes and phases of the constituents previously considered as well established did not change appreciably. As an example, we concluded the analysis before Berdnikov reported a new series of photoelectric data (Berdnikov et al. 1995a, 1995b; Berdnikov & Turner 1995a, 1995b), but we felt us obliged to revise the results obtained so far (reported in Pardo 1995). This further extension of the available data strengthened our confidence since it did not produce any significant numerical change; the only, but remarkable, exception was to give stronger evidence of the  $2f_2$  and  $3f_1$  terms in the light curve of EW Sct.

The whole sets of data used for the analysis can be requested from the authors.

## 4. Star by star

In this section we shortly review each star, reporting a detailed description for BQ Ser and AX Vel only; a thorough discussion of the frequency and least-squares analysis of all the DMCs was performed by Pardo (1995). In the discussion we used the phase differences  $\phi_{21} = \phi_2 - 2\phi_1$  and  $\phi_{31} = \phi_3 - 3\phi_1$  (which can be calculated for both the  $f_1$  and  $f_2$  terms); the discussion of the *generalized phase differences* will take place in Paper II. Table 2 summarizes the general results obtained on all the DMCs. We report below (Subsect. 4.1) the full application of our procedure to the BQ Ser measurements and Tab. 3 shows the results obtained step by step. Tables 4 and 5 list the Fourier coefficients of the fits of the whole sets of data for the 14 other stars.

### 4.1. BQ Ser

The full analysis of this star is described in Tab. 3; let us examine it in detail. The preliminary analyses of the three subsets yielded some slight differences in the frequency content. Firstly, the BERD subset (upper part, right panel) evidenced the  $2f_2$  term, but this term was not detected by the frequency analysis of the other subsets; however, a forced fit on the LTPV data (upper part, middle panel) yield a very similar phase value (between brackets; note that the  $T_0$ 's are the same) and this term was considered as real. Then, the LTPV and BERD subsets were merged into one dataset (the measurements were performed in the same years) and its frequency analysis evidenced once again the same terms (lower part, middle panel), thus confirming their agreement in phase. Now, we can compare the LTPV+BERD dataset with the MB84 one, where the  $2f_2$  and  $3f_1$  terms were not detected (upper part, left panel). When these terms were added in the forced least-squares fit of the MB84 data, the parameters of the fit did not change appreciably (compare the upper and lower right panels of Tab. 3) and we obtained Fourier parameters ( $\phi_{21}=4.98\pm0.95$  rad for the  $f_2$  term and  $\phi_{31}=2.71\pm1.70$  rad for the  $f_1$  term) very similar to those obtained by fitting the LTPV+BERD data ( $5.26\pm0.19$  rad and  $2.35\pm0.18$  rad, respectively). Considering all the terms, the maximum difference between the amplitudes is 0.004 mag, within the formal error bars. Therefore we can conclude that the light curve of BQ Ser contains the  $f_1$ ,  $f_2$ ,  $2f_1$ ,  $f_1 + f_2$ ,  $f_2 - f_1$ ,  $2f_2$ ,  $3f_1$ ,  $2f_1 + f_2$  terms. The right panel of the lower part of Tab. 3 lists the parameters of the final fit on all the available data (the BERD measurements obtained by using a different equipment (Berdnikov & Turner 1995a, 1995b) were added to the previous ones). It is useful to verify once again that the phase and amplitude values of the final fit are very similar to those of the fit of the BERD subset, as should happen when adding measurements with the same

**Table 3.** The complete analysis of BQ Ser data. The MB84, BERD, LTPV subsets were analyzed separately (upper panels); then the last two were merged into the LTPV+BERD dataset (middle panel in the lower part). A fit was forced on the MB84 data to check the phase values of undetected terms (left panel in the lower part); since the check was positive (see text to compare phase difference values), all the terms were included in the global fit (right panel in the lower part)

Term	Frequency [cd <sup>-1</sup> ]	Ampl. [mmag]	Phase [rad 10 <sup>-2</sup> ]	Frequency [cd <sup>-1</sup> ]	Ampl. [mmag]	Phase [rad 10 <sup>-2</sup> ]	Frequency [cd <sup>-1</sup> ]	Ampl. [mmag]	Phase [rad 10 <sup>-2</sup> ]
	Subset: MB84			Subset: LTPV			Subset: BERD		
$f_1$	0.234140	176±3	56±2	0.234143	179±2	155±2	0.234136	176±1	157±1
$f_2$	0.332020	109±2	109±2	0.331985	112±3	232±2	0.331999	111±1	236±1
$2f_1$		34±3	535±9		29±3	91±10		31±1	110±4
$f_1+f_2$		38±2	618±9		36±3	210±8		36±1	214±4
$f_2-f_1$		18±2	526±12		20±3	535±14		20±1	532±7
$2f_2$					(5±2)	(328±64)		5±1	364±26
$3f_1$					6±3	19±49		6±1	75±26
$2f_1+f_2$		12±3	446±25		9±2	168±34		7±1	154±20
$V_0$	9.5137±0.0015			9.5139±0.0015			9.5110±0.0009		
rms	0.0126 mag			0.0157 mag			0.0169 mag		
N	81			121			367		
$T_0$	HJD 2444397.3965			HJD 2448199.2453			HJD 2448199.2453		
	Dataset: MB84			Dataset: LTPV + BERD			Whole set		
$f_1$	0.234140	174±3	55±2	0.234137	177±1	156±1	0.234138	177±1	155±1
$f_2$	0.332020	112±4	110±3	0.331999	112±1	235±1	0.331997	112±1	236±1
$2f_1$		32±3	536±10		30±1	105±4		31±1	103±3
$f_1+f_2$		38±3	612±10		36±1	212±3		36±1	213±2
$f_2-f_1$		19±2	524±12		20±1	534±6		20±1	537±4
$2f_2$		(4±4)	(90±93)		5±1	363±23		5±1	367±19
$3f_1$		(3±5)	(436±168)		6±1	62±18		6±1	67±16
$2f_1+f_2$		11±4	452±31		7±1	157±15		9±1	152±10
$V_0$	9.5133±0.0016			9.5110±0.0008			9.5107±0.0006		
rms	0.0125 mag			0.0167 mag			0.0149 mag		
N	81			488			602		
$T_0$	HJD 2444397.3965			HJD 2448199.2453			HJD 2448199.2453		

frequency content. The  $f_1$  and  $f_2$  values are practically co-incident (over a 11-year basis).

Figure 3 shows the light curves of the two periods of BQ Ser: the upper curve was obtained by subtracting the  $f_2$ ,  $2f_2$ ,  $f_1+f_2$ ,  $f_2-f_1$ ,  $2f_1+f_2$  terms from the measurements (whole set of data), the lower one by subtracting  $f_1$ ,  $2f_1$ ,  $3f_1$ ,  $f_1+f_2$ ,  $f_2-f_1$ ,  $2f_1+f_2$ . To fit the upper curve two harmonics are necessary, while the first harmonic is sufficient to fit the lower curve. If the order of the fit had been established *a priori*, the same harmonic contents would have been used, but this assumption was not justified by the different shapes of the two light curves.

Szabados (1993) claimed evidence for a third periodicity ( $f_3=0.42$  cd<sup>-1</sup>) in the light curve of BQ Ser on the basis of his unpublished data. However, it must be noted that the very common  $2f_2$  harmonic was not detected and that its value (0.66 cd<sup>-1</sup>) is very close to one of the largest amplitude terms involving the  $f_3$  term (0.65 cd<sup>-1</sup>). Hence,

in our opinion, the  $f_3$  term detection arose from a misidentification of the  $2f_2$  component in an early step of the frequency analysis; it should be noted that a plausible explanation for the 0.42 cd<sup>-1</sup> term itself is the identification of the  $2f_2-f_1$  term (0.43 cd<sup>-1</sup>).

#### 4.2. AX Vel

As a further example of the procedure reported above, the analysis of AX Vel allows us to give a better description of some other aspect. We preliminarily scrutinized the three available subsets (BA83, P76, SB79), calculating the mean magnitudes of each of them (8.213, 8.219, 8.215, respectively) and then we merged the last two into one (PSB dataset). By performing the careful frequency analysis described in section 2, in both datasets we detected the  $f_1$ ,  $f_2$ ,  $f_2-f_1$ ,  $f_1+f_2$ ,  $2f_1$ ,  $2f_2$  terms. The frequency analysis of BA83 dataset also evidenced the  $2f_1+f_2$  terms, while that of the PSB dataset evidenced the  $3f_1$  term. To check

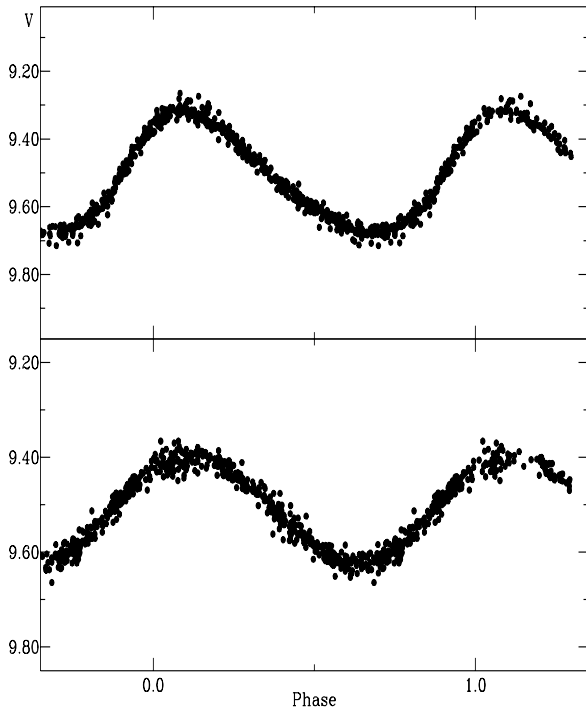


**Fig. 3.** Light curves of the two independent frequencies  $f_1 = 0.234138 \text{ cd}^{-1}$  (upper panel) and  $f_2 = 0.331997 \text{ cd}^{-1}$  (lower panel) as obtained from the whole BQ Ser set of data

if these two terms have a physical meaning, we applied a least-squares fit separately to both datasets by using all the above quoted terms. As a result, in the PSB dataset the  $2f_1 + f_2$  term had a phase value of  $3.1 \pm 0.3$  rad (against  $2.6 \pm 0.3$  rad obtained in the Barrell dataset); since the two values are similar and error bars are overlapping, this term is included in the light curve content of AX Vel. On the other hand, the fit of the BA83 subset considering also the  $3f_1$  term yielded a large error bar on the phase value of this term (i.e.  $\pm 2.6$  rad), preventing a reliable confirmation; hence, this term was dropped from the final least-squares solution. When this analysis was concluded, Berdnikov & Turner (1995) reported on new measurements (26): they were not sufficient to perform a reliable frequency analysis, but by adding this subset we improved the frequency values (the time baseline being much longer) and then we included it in the whole set of data.

AX Vel resulted to be the only DMC having the  $f_2$  amplitude larger than the  $f_1$  one. The rms residuals of the subsets are small (0.007 and 0.010 mag for BA83 and

PSB, respectively) and this allowed us to detect the shallow  $2f_1$  term. It is important to note, once more, that also in the case of this small amplitude term the Fourier decomposition supplies coherent and meaningful results: the BA83 dataset yielded  $\phi_{21} = 4.0 \pm 0.3$  rad, while the PSB dataset yields  $\phi_{21} = 4.4 \pm 0.2$  rad.

The comparison between the frequency values suggests to us a very stable behaviour of AX Vel. On the other hand, the amplitudes of the two frequencies are different in the two datasets. This fact has two consequences: the rms residual of the whole set is slightly higher than that of each dataset and some signal is left at the  $f_1$  and  $f_2$  values in the final power spectrum. We cannot be sure that this difference has a physical origin, since the measurements were collected in different photometric systems (*uvby*, *UBV*, *VBLUW*, ...) and instrumental and/or transformation effects can originate the small (no more than 0.010 mag) discrepancies observed.

#### 4.3. AP Vel

Similarly to AX Vel, we merged the three available subsets into two: the first was composed by the LTPV data only, the second was formed by grouping the SB79 and P76 measurements. By comparing the results obtained with the two different datasets, the very small differences found in the amplitude values were considered as not significant. The frequency analysis allowed us to detect the  $f_1$ ,  $f_2$ ,  $f_2 - f_1$ ,  $f_1 + f_2$ ,  $2f_1$ ,  $2f_2$ ,  $3f_1$ ,  $2f_1 + f_2$  terms; the  $2f_2 + f_1$  and  $3f_1 + f_2$  terms were detected in one dataset and confirmed by the forced fit on the other. On the other hand, the small amplitude terms  $4f_1$ ,  $4f_1 + f_2$  were not considered since the phase values were in disagreement. In the final fit of the whole set of data (10 terms) we also added the BERD measurements.

#### 4.4. TU Cas

The frequency analysis of the long term photometry of this DMC should give an important answer about period variations. We separately analyzed three large subsets (OO59, WE57, BERD), spanning 50 years. The results do not support any trace of period variability: we found, respectively, 0.46747, 0.46746, 0.46745  $\text{cd}^{-1}$  for  $f_1$  (error bar:  $\pm 0.00001 \text{ cd}^{-1}$ ), 0.65859, 0.65860, 0.65864  $\text{cd}^{-1}$  (error bar:  $\pm 0.00002 \text{ cd}^{-1}$ ) for  $f_2$ . As regards the amplitudes, the values determined in the WE57 subset are appreciably larger than the others (0.32 mag for  $f_1$ , 0.14 mag for  $f_2$  against 0.29 mag and 0.10, respectively), but the physical meaning of this fact should be considered with caution owing to instrumental differences. As a consequence, the last power spectrum shows some residual signal around the  $f_1$  and  $f_2$  values. The OO59 dataset was not included in the global set owing to its large scatter (0.061 mag). Also the Matthews et al. data (1992) could not be included, since its spectral window is very bad: this fact hampered



a careful frequency analysis and misleading results were obtained when forcing a fit.

The presence of a third period in the light curve of TU Cas is a controversial point: false alarms are recurring in the DMC literature. In agreement with the most recent results (Matthews et al. 1992), we did not find any trace of this third period.

#### 4.5. *U TrA*

Six subsets were available (OO57, MI64, JA62, FS79, SB79, BERD) and they were grouped into three datasets. However, the dataset constituted by the MI64 and OO57 measurements showed a large scatter (more than 0.04 mag) and it was used only to check the period values, which seem to be very stable; only the  $f_1$  value obtained from the JA62 measurements ( $0.38947 \pm 0.00009 \text{ cd}^{-1}$ ) is marginally different from the other two ( $0.38934 \pm 0.00001$  and  $0.38933 \pm 0.00002 \text{ cd}^{-1}$ ). As a consequence, the last power spectrum shows some residual signal around the  $f_1$  value.

#### 4.6. *EW Sct*

Figer et al. (1991; LTPV and Merate Observatory measurements) already reported a Fourier decomposition obtained by using the procedure applied here to all the DMCs; in addition, we now have at our disposal the 400 measurements collected by BERD. The decomposition of the BERD data allowed us to detect the  $2f_2$ ,  $2f_1 + f_2$  and  $3f_1$  terms, whose phase values were confirmed by the forced fit on Figer et al.'s data. However, a small difference in the amplitude of the  $f_1$  and  $f_2$  terms is observed when comparing the FP91 and BERD subsets; the difference is particularly significant for the  $f_2$  term (0.114 mag in the FP91 data, 0.127 in the BERD one) and may suggest a physical variation. As a consequence, the last power spectrum shows some residual signal at values close to the  $f_2$  value.

#### 4.7. *VX Pup*

The frequency analysis of the datasets obtained by merging the SB79 and MB84 measurements and considering the LTPV data only are very similar; amplitude and frequency values are within the error bars. The  $f_1$ ,  $f_2$ ,  $f_2 - f_1$ ,  $f_1 + f_2$ ,  $2f_1$ ,  $2f_2$ ,  $3f_1$ ,  $2f_1 + f_2$ ,  $2f_2 + f_1$  are detected in both datasets; the  $2f_2 - f_1$  term only in the LTPV dataset, but its reality was confirmed. The phases of the  $3f_1 + f_2$  term are only marginally coincident, but the power spectrum obtained by introducing all the above terms clearly showed it and therefore it was considered in the global fit, which also considered the BERD measurements. It should be noted that the two close terms  $f_2 - f_1 = 0.1353 \text{ cd}^{-1}$  and  $2f_1 - f_2 = 0.1314 \text{ cd}^{-1}$  are both observed in the power spectra.

#### 4.8. *Y Car*

The available data were firstly grouped into two datasets (SB79+P76, BERD). The frequency analysis allows us to detect the  $f_1$ ,  $f_2$ ,  $f_2 - f_1$ ,  $f_1 + f_2$ ,  $2f_1$ ,  $2f_2$ ,  $3f_1$ ,  $2f_1 - f_2$ ,  $2f_2 + f_1$ ,  $3f_1 + f_2$ . SB79 only considered the first six terms: the identification of the other terms allowed us to reduce the rms residual from 0.024 mag to 0.017 mag. When forming the whole set of data, the rms again increased to 0.021 mag, owing to the lesser accuracy of the BERD data. The last power spectrum is very noisy and a peak at  $0.94 \text{ cd}^{-1}$  (or  $1.06 \text{ cd}^{-1}$ ) is visible; since the two coupling terms  $0.940182 \text{ cd}^{-1}(2f_1 + f_2)$  and  $1.056138 \text{ cd}^{-1}(f_1 + 2f_2)$  were already considered, its nature is not obvious. However, the number of measurements is quite small and these results can be an artifact due to poor sampling.

#### 4.9. *AS Cas*

The photoelectric measurements carried out by BERD do not have the same mean magnitude from one year to the next; first, they were aligned to the same value (maximum correction: 0.086 mag) before performing the frequency analysis described in Sect. 2. In spite of this, a spurious peak was detected at  $1.002 \text{ cd}^{-1}$ . The rms residual (0.028 mag) is high (in particular the measurements reported by Berdnikov et al. 1995 display a large scatter), but it should be noticed that AS Cas has a mean magnitude  $V=12.26$  and that it was observed with a 60-cm reflector.

#### 4.10. *BK Cen*

The precision of the measurements in the available subsets (LJ65, SB79, LTPV and BERD) is different. We analyzed them separately and we found very similar amplitude and phase values, confirming the internal stability of the proposed solution. In particular, the frequency analysis of the LJ65 and LTPV subsets yielded  $f_1$  and  $f_2$  values coincident within error bars, suggesting no period variation over more than 30 years. The rms residual (0.0231 mag) and the residual noise amplitude are rather high (0.004 mag). This can be due to a high number of measurements with a residual between  $3\sigma$  and  $4\sigma$  which we preferred not to delete.

#### 4.11. *V367 Sct*

To perform photometric measurements of this faint DMC belonging to the open cluster NGC 6649 is not an easy task, but the last power spectrum did not show any residual high level peak. Even if large error bars prevent a detailed analysis, frequency and amplitude values seems to be stable in the three available subsets (MS78, MV75, BERD): the  $f_1$ ,  $f_2$ ,  $f_2 - f_1$ ,  $f_1 + f_2$ ,  $2f_1$ ,  $2f_2$  terms are detected in all the subsets. The small amplitude  $3f_1$  term was firstly detected in the BERD subset and then confirmed by the fit on the other subsets.

#### 4.12. GZ Car

The frequency analysis was carried out by combining the SB79 and P76 subsets; despite the small number of measurements (91), the harmonics  $2f$  of both frequencies, the coupling terms  $f_2 - f_1$  and  $f_1 + f_2$  and the  $2f_1 + f_2$  were found. The detection of the small amplitude  $2f_2$  term is notable. To have a solution based on a higher number of points, the BERD subset was added.

#### 4.13. UZ Cen

We performed the frequency analysis by combining the SB79 and P76 subsets. As in the case of AP Vel, the BERD subset was added to perform the global fit. The  $f_1$  light curve is very asymmetrical (3 harmonics are required); on the other hand, the  $f_2$  amplitude is the smallest observed in the whole sample and the shallow  $2f_2$  term was detected only in the last steps of the analysis.

#### 4.14. CO Aur

The three subsets (AM84+AM86, BB87, BERD; in the latter the annual misalignment was corrected) yield very similar results for amplitude and frequency values. It is important to note that the  $2f_2$  term cannot be detected in a reliable way and hence the light curve on  $f_2$  must be considered to be sine-shaped. In addition to  $f_1$ ,  $f_2$ ,  $2f_1$ , the terms  $f_1 + f_2$ ,  $f_2 - f_1$ ,  $3f_1$  can be detected.

### 5. Discussion and Conclusions

The frequency analysis performed by the least-squares method allowed us to obtain a very detailed description of the light curves of the galactic DMCs. With respect to the goals of this first investigation, some conclusions can be extracted directly from the analysis reported in the previous section:

1. The 2<sup>nd</sup> order terms are present in the light curves of all the stars, but in every case a fit limited to the 2<sup>nd</sup> order is not satisfactory. As regards the  $f_1$  component, only AX Vel and GZ Car do not show the  $3f_1$  harmonic, while TU Cas, U TrA and UZ Cen show also the 4<sup>th</sup> harmonic. As regards the  $f_2$  component, only the first harmonic is observed in its light curve. The coupling terms are observed in a large variety of combinations. The  $f_1 + f_2$  and  $f_2 - f_1$  terms are observed in all the stars and also the  $2f_1 + f_2$  term is rather common. Curiously, Alcock et al. (1995) and Welch et al. (1996) presented only the 2<sup>nd</sup> order components in their discussion of DMC light curves in the LMC; probably a deeper analysis can yield some other interesting results.
2. The two independent frequencies  $f_1$  and  $f_2$  seem to be very stable, in the sense that a reasonable fit can be obtained without admitting their variation. U TrA is the most promising candidate to show such a variation,

since a slightly different  $f_1$  value was obtained for the oldest subset;

3. In none of the stars a convincing third independent periodicity is detected, even in the cases of TU Cas and BQ Ser, the two claimed candidates;
4. The amplitudes of the modes do not show variations exceeding the error bars, with the exception of the  $f_2$  term in the EW Sct light curve; this star is the most suitable target for an extensive long-term photometry project carried out by using a very stable instrumentation. Berdnikov (1992) showed how the light curve changes in amplitude over a period when considering different phases of the other period. However, this effect is not real, since it is due to the presence of the cross coupling terms, which Berdnikov did not subtract from the original measurements; when considering these terms, light curves with constant amplitude over each period can be easily constructed, as Fig. 3 shows for BQ Ser. A full set of light curves over the two periods for each DMC can be found in Pardo (1995).

In Introduction we mentioned the separation between Classical and  $s$ -Cepheids in the space of Fourier parameters; Antonello et al. (1990) ascribed this separation to the different pulsation mode and also invoked the action of a resonance at or near 3.0 d to explain the “Z” shape of the  $s$ -Cepheid progression. The very reliable Fourier parameters now at our disposal for the galactic DMCs allow us to give an independent confirmation of these interpretations. Figure 4 shows the distribution of the  $\phi_{21}$  values of the galactic DMCs superimposed to the Classical and  $s$ -Cepheids ones. The  $\phi_{21}$  values corresponding to the  $F$  radial mode occupy the same region as the Classical Cepheids. In like manner, the  $\phi_{21}$  values of the  $1O$  radial mode mimics the “Z” shape: note the overlap between DMCs and  $s$ -Cepheids in the upper part, the high value at 3.0 d (BQ Ser) and the positioning of the two  $\phi_{21}$  values belonging to the longest period DMCs (EW and V367 Sct) just on the lower part. It appears quite evident that in the DMCs the light curves of the  $F$ -radial mode and the  $1O$ -mode are very similar to the curves of the Classical and  $s$ -Cepheids, respectively. In turn, this fact proves without any doubt that  $s$ -Cepheids are pulsating in the  $1O$  mode and that the  $\phi_{21}$  value can be considered a powerful discriminant between these modes. It should be also noted that the  $F$ -mode light curve follows the Hertzsprung progression. A discontinuity is present near 3.0 d in the light curves of  $1O$  pulsators and a resonance effect is the more likely cause.

The case of CO Aur deserves a particular attention. The ratio between the observed frequencies is 0.800 and this value is explained by the excitation of the  $1O$  and  $2O$  modes. In the  $\phi_{21}$ - $P$  plane the  $\phi_{21}$  value for the  $f_1$  term falls in the short period region, where the  $1O$  and  $F$  sequences are merging; we can only conclude that the  $\phi_{21}$  value for this unique (in the Galaxy) pulsator is quite similar to the others. It has not been possible to detect the

**Table 4.** Coefficients of the least-squares fits of the whole sets of data: TU Cas, U TrA, UZ Cen, AS Cas, VX Pup, BK Cen, AP Vel, Y Car, EW Sct

Term	Frequency [cd <sup>-1</sup> ]	Ampl. [mmag]	Phase [rad 10 <sup>-2</sup> ]	Frequency [cd <sup>-1</sup> ]	Ampl. [mmag]	Phase [rad 10 <sup>-2</sup> ]	Frequency [cd <sup>-1</sup> ]	Ampl. [mmag]	Phase [rad 10 <sup>-2</sup> ]
	TU Cas			U TrA			UZ Cen		
$f_1$	0.467442	292±1	431±1	0.389344	263±1	520±1	0.299910	291±3	16±1
$f_2$	0.658635	114±1	219±2	0.547983	101±1	625±1	0.424589	82±3	623±4
$2f_1$		101±1	21±1		85±1	199±1		95±3	454±4
$f_1 + f_2$		78±1	413±1		65±1	293±1		54±3	428±6
$f_2 - f_1$		37±1	192±3		26±1	479±4		21±3	405±15
$2f_2$		14±1	243±8		10±2	433±8		10±3	439±31
$3f_1$		37±1	244±3		28±1	512±3		41±3	267±7
$2f_1 + f_2$		49±1	14±2		46±2	601±2		32±3	255±9
$f_1 + 2f_2$		19±1	419±6		15±1	67±6			
$2f_2 - f_1$		7±1	172±16						
$4f_1$		12±1	444±9		9±1	156±9		14±3	82±22
$3f_1 + f_2$		23±1	236±4		19±2	296±4		22±3	52±14
$2f_1 + 2f_2$		15±1	2±7						
$3f_1 - f_2$								7±3	105±45
$3f_1 + 2f_2$		7±1	211±14						
$4f_1 + f_2$		11±1	445±9		9±1	600±10			
$V_0$		7.7687±0.0007			7.9695±0.0006			8.8000±0.0018	
rms		0.0161 mag			0.0167 mag			0.0190 mag	
N		618			1060			131	
$T_0$		HJD 2448752.3129			HJD 2436764.8808			HJD 2442125.1938	
	AS Cas			VX Pup			BK Cen		
$f_1$	0.330628	203±2	90±1	0.332030	174±1	186±1	0.315072	266±2	39±1
$f_2$	0.463936	137±2	242±1	0.467384	144±1	408±1	0.449860	108±2	116±2
$2f_1$		62±2	595±3		32±1	158±6		70±2	501±3
$f_1 + f_2$		67±2	116±2		51±1	380±3		54±2	582±4
$f_2 - f_1$		35±2	561±5		25±1	44±7		26±2	521±8
$2f_2$		19±2	290±9		17±1	7±11		11±2	92±19
$3f_1$		16±2	489±12		7±1	161±30		26±2	325±8
$2f_1 + f_2$		36±2	4±5		19±1	358±10		32±2	408±6
$f_1 + 2f_2$		19±2	189±9		12±1	602±14		11±2	500±18
$2f_2 - f_1$		11±2	613±15		7±1	240±22			
$3f_1 + f_2$		16±2	513±11		5±1	378±30		11±2	226±19
$V_0$		12.2689±0.0015			8.3201±0.0008			10.1333±0.0015	
rms		0.0265 mag			0.0121 mag			0.0231 mag	
N		575			234			251	
$T_0$		HJD 2448648.4725			HJD 2443803.1587			HJD 2446319.7188	
	AP Vel			Y Car			EW Sct		
$f_1$	0.319717	279±1	334±1	0.274742	265±3	311±1	0.171719	171±1	432±1
$f_2$	0.454587	137±1	485±1	0.390698	117±3	518±2	0.245820	124±2	212±1
$2f_1$		79±1	457±2		79±3	412±4		28±2	48±6
$f_1 + f_2$		52±2	587±3		68±3	628±4		31±1	485±6
$f_2 - f_1$		36±1	592±4		32±3	37±10		20±2	249±8
$2f_2$		16±2	159±11		12±3	213±22		5±2	96±32
$3f_1$		26±2	604±6		28±3	531±10		40±1	295±50
$2f_1 + f_2$		28±2	509±6		21±3	108±13		57±2	54±30
$f_1 + 2f_2$		12±2	250±14		9±3	318±31			
$3f_1 + f_2$		6±1	191±23		14±3	205±21			
$V_0$		10.0610±0.0010			8.1080±0.0020			7.9888±0.0007	
rms		0.0158 mag			0.0213 mag			0.0165 mag	
N		255			137			515	
$T_0$		HJD 2446298.5843			HJD 2442250.5989			HJD 2446300.2641	

**Table 5.** Coefficients of the least-squares fits of the whole sets of data: AX Vel, GZ Car, V367 Sct, CO Aur. For BQ Ser see the last panel of Tab. 3

Term	Frequency [cd <sup>-1</sup> ]	Ampl. [mmag]	Phase [rad 10 <sup>-2</sup> ]	Frequency [cd <sup>-1</sup> ]	Ampl. [mmag]	Phase [rad 10 <sup>-2</sup> ]
AX Vel			GZ Car			
$f_1$	0.272241	106±1	23±1	0.240448	147±2	265±1
$f_2$	0.385657	143±1	469±1	0.390698	87±2	62±2
$2f_1$		11±2	463±7		23±2	335±8
$f_1 + f_2$		28±1	300±3		25±2	152±7
$f_2 - f_1$		12±1	284±7		16±2	225±11
$2f_2$		11±1	138±8		4±2	594±45
$2f_1+f_2$		6±1	170±15			
$2f_2-f_1$					8±2	24±22
$V_0$	8.2148±0.0007			10.2387±0.0013		
rms	0.0109 mag			0.0130 mag		
N	520			118		
$T_0$	HJD 2443892.0164			HJD 2442073.2970		
V367 Sct			CO Aur			
$f_1$	0.158902	176±1	542±1	0.560844	173±1	288±1
$f_2$	0.228061	117±1	203±1	0.700390	43±2	233±4
$2f_1$		27±1	278±5		31±1	357±6
$f_1 + f_2$		18±1	519±7		9±1	345±19
$f_2 - f_1$		15±1	160±9		7±2	418±23
$2f_2$		14±1	140±10			
$3f_1$		4±1	588±33		7±2	419±26
$V_0$	11.6073±0.0009			7.7142±0.0008		
rms	0.0207 mag			0.0146 mag		
N	514			370		
$T_0$	HJD 2448093.7156			HJD 2445758.3582		

$2f_2$  term, i.e. the  $f_2$  light curve is perfectly sine-shaped. Stellingwerf et al. (1987) predicted an asymmetrical light curve for a 2O pulsator, but this does not seem to be verified in the CO Aur case. It should also be noted that between the single-mode Cepheids there are two stars (V1334 Cyg and DT Cyg) showing a perfectly sine-shaped light curve (Poretti 1994). In view of the close similarity evidenced above between single and double-mode pulsators, further investigation of the pulsating mode of V1334 Cyg and DT Cyg is recommended.

*Acknowledgements.* The authors wish to thank E. Antonello, L. Mantegazza, L. Pasinetti for useful discussions and J. Vialle for the improvement of the English form of the manuscript.

## References

Alcock C., et al. (MACHO project Team), 1996, *AJ*, 109, 1653  
 Antonello E., Mantegazza L., 1984, *A&A* 133, 52  
 Antonello E., Mantegazza L., Poretti E., 1986, *A&A* 159, 269  
 Babel J., Burki G., 1987, *A&A* 181, 34  
 Barrell S.L., 1983, *MNRAS* 204, 1

Beaulieu J.P., et al. (EROS project Team), 1995, *A&A* 303, 137  
 Berdnikov L.N., 1992, *SvA Letters* 18, 259  
 Berdnikov L.N., 1993, *SvA Letters* 19, 84  
 Berdnikov L.N., Turner D.G., 1995a, *Pis'ma Astr. Zhurnal* 21, 803  
 Berdnikov L.N., Turner D.G., 1995b, *Pis'ma Astr. Zhurnal* 21, in press  
 Berdnikov L.N., Voziakova O.V., Ibragimov M.A., 1995a, *IAU Inform. Bull. Var. Stars* 4141  
 Berdnikov L., Voziakova O.V., Ibragimov M.A., 1995b, *IAU Inform. Bull. Var. Stars* 4142  
 Carpino M., Milani A., Nobili A.M., 1987, *A&A* 181, 182  
 Faulkner D.J., Shobbrook R.R., 1979, *ApJ* 232, 197  
 Figier A., Poretti E., Sterken C., Walker N., 1991, *MNRAS* 249, 563  
 Jansen A.G., 1962, *Bull. Astr. Nether.* 16, 141  
 Manfroid J., Sterken C., et al., 1991, *ESO Scientific Report* 8  
 Manfroid J., Sterken C., et al., 1994, *ESO Scientific Report* 14  
 Mantegazza L., Poretti E., 1992, *A&A* 261, 137  
 Matthews J.M., Gieren W.P., Fernie J.P., Dinshaw N., 1992, *AJ* 104, 748

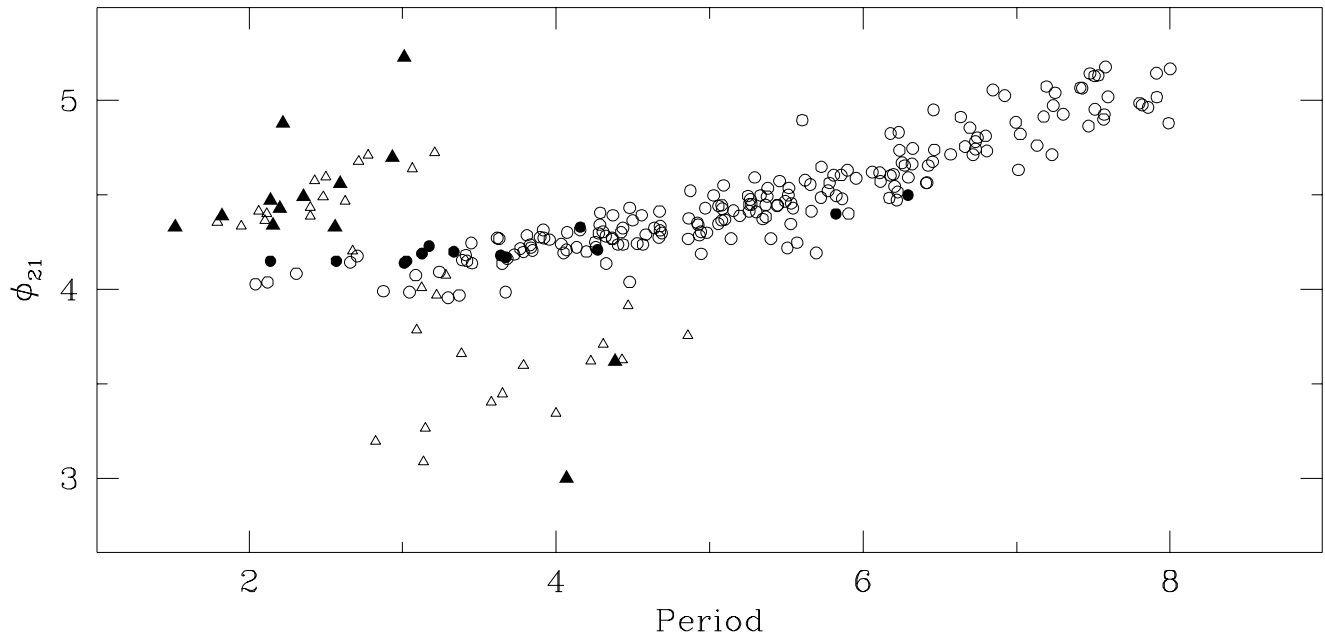


**Fig. 4.** The  $\phi_{21}$ – $P$  plane. Dots: single-mode Classical Cepheids. Triangles:  $s$ -Cepheids. Filled dots: Fundamental radial mode of DMCs. Filled triangles:  $1O$  radial mode of DMCs.

- Mitchell R.I., Iriarte B., Steinmetz D., Johnson H.L., 1964,  
 Boll. Obs. Tonantzintla y Tacubaya 3, 153  
 Moffett T.J., Barnes T.G., 1984, ApJS 55, 389  
 Oosterhoof P.T., 1957, Bull. Astr. Nether. 13, 320  
 Oosterhoof P.T., 1959, Bull. Astr. Nether. 15, 204  
 Pardo I., 1995, (in Italian), Laurea Thesis, Università di Milano  
 Pel J.W., 1976, AAS 26, 413  
 Poretti E., 1994 A&A 285, 524  
 Poretti E., Pardo I., 1996, A&A, submitted (Paper II)  
 Schmidt E.G., Chab J.R., Reiswig D.E., 1995, AJ 109, 1239  
 Stellingwerf R.F., Gautschi A., Dickens R., 1987, ApJ 313, L75  
 Sterken C., Manfroid J., et al., 1993, ESO Scientific Report 12  
 Stobie R.S., Balona L.A., 1979, MNRAS 188, 595  
 Stobie R.S., Balona L.A., 1979, MNRAS 189, 627  
 Szabados L., 1993, in *Applications of Time Series Analysis in  
 Astronomy and Meteorology*, Università di Padova, Sept. 6–  
 10, 1993  
 Vaniček P., 1971, ApSS 12, 10  
 Welch et al., 12<sup>th</sup> IAP Colloquium, Paris, 1996 July, in press  
 Worley C.E., Eggen O.J., 1957, AJ 62, 104